Stochastic exposure kinetics of extreme ultraviolet photoresists: Trapping model

Chris A. Mack[a)]
Lithoguru.com, 1605 Watchhill Rd., Austin, Texas 78703

John J. Biafore and Mark D. Smith
KLA-Tencor, FINLE Division, 8843 N. Capital of Texas Highway, Austin, Texas 78759

(Received 21 June 2013; accepted 16 September 2013; published 1 October 2013)

The mechanism of extreme ultraviolet resist exposure is still in debate, with various competing mechanisms proposed. Here, three different continuum exposure models and two stochastic exposure models are compared, using predictions of acid concentration and yield as a function of dose and photoacid generator (PAG) loading. The models studied are a stochastic excitation model (and its continuum counterpart), a stochastic PAG trapping model (and its newly derived continuum counterpart), and the continuum Higgins competing traps model. These models produce different predictions for acid concentration as a function of dose and PAG loading, and for acid yield as a function of PAG loading. Thus, it may be possible to use experimental data to differentiate between these mechanisms, though the possibility of multiple simultaneous mechanisms cannot be ruled out.
 [http://dx.doi.org/10.1116/1.4823759]

I. INTRODUCTION

Unlike the direct photolysis mechanism of exposure for 248- and 193-nm photoresists, extreme ultraviolet (EUV) resists are exposed via photoionization: a high-energy photon absorbed in the resist ionizes the polymer, generating an electron (called a photoelectron), which in turn can generate several secondary electrons.[1,2] These electrons then scatter through the resist losing energy and, occasionally, interacting with a photoacid generator (PAG) to generate an acid. While there have been many proposals, there is no universally accepted mechanism for how the electron interacts with the PAG. The two main proposals are electronic excitation and dissociative electron attachment (trapping).

In a typical excitation mechanism (similar to that used for many years in electron-beam lithography simulation[3]), an electron transfers energy to a PAG while passing close by. The electron is not consumed in this interaction and can continue on its path, possibly exciting other PAGs. In a trapping mechanism, the electron must be trapped by the PAG in order to excite it and is thus consumed in the reaction. Additionally, other species could also trap the electron, competing with the PAG. The behavior of the electron as it travels through the resist also impacts its ability to cause acid generation: scattering, energy loss, secondary electron generation, and inert trapping. As we shall see below, these different mechanisms lead to different exposure behaviors. It is the goal of this paper to explore the predictions made by a few different models employing these different excitation mechanisms.

Two basic modeling approaches will be used to describe EUV resist exposure: continuum kinetics and stochastic Monte Carlo-like numerical simulations. First, standard continuum kinetics techniques will be used to derive rate equations for each of the three mechanisms studied here. Two of these kinetic rate equations have been previously derived, and a third one will be derived below. Then, the PROLITH Stochastic Resist Model (SRM) (version X4.2, from KLA-Tencor) will be used to model the mean acid concentration after exposure for the simple case of a large open-frame exposure for two of these mechanisms. By finding the mean acid concentration as a function of exposure dose, the exposure rate behavior of an EUV resist can be extracted as a function of the stochastic resist parameters for different mechanisms. PROLITH includes both excitation and trapping exposure mechanisms, as will be detailed below, and these mechanisms can be individually turned on or off.

Here, three different exposure mechanisms will be explored: excitation, PAG trapping alone, and PAG trapping with competing traps. Two of the mechanisms have been implemented as stochastic models, with continuum kinetic models derived as well. One mechanism (the competing traps model) is only studied as a continuum kinetic model. Predictions of the models include the shape of the acid versus dose curve, the impact of initial PAG concentration on the shape of that curve, and the impact of initial PAG concentration on the initial acid yield. Differences in these predictions can lead to the development of experiments that might discriminate between the different models.

II. EXCITATION MODEL

The stochastic EUV resist models of the PROLITH SRM do not assume a first-order exposure mechanism, but instead simulate a sequence of more elementary steps that lead to the generation of an acid.[2] Photons with a Poisson distribution strike the resist film. The probability of absorption in the resist is determined by Lambert's law (in this study, the direct photolytic mechanism for conversion of PAG is disabled). Once a photon has been absorbed, one electron is released with probability ϕ_e (the photoelectron generation efficiency), and with kinetic energy equal to the photon

[a)]Electronic mail: chris@Lithoguru.com

energy minus the ionization potential, *IP*. The primary photoelectron then travels and scatters through the resist, possibly inducing further ionization and resulting in a cascade of secondary electrons. As the electrons travel through the resist they lose kinetic energy continuously (in a typical *continuous slowing-down approximation*).[4,5] The stopping power of the resist is the energy lost by an electron per unit path length traveled and is calculated with the complex dielectric function for a model compound (polystyrene, C_8H_8).[6,7] Photoacid generators are randomly dispersed throughout the resist in a Poisson distribution with average density P_0.

This mechanism of photoelectron and secondary electron generation is assumed to be true for all of the models studied here. The interaction of the electrons with the PAG differs per model. For the case of the excitation mechanism, electrons that pass within the excitation reaction radius (r) of a PAG may transfer enough energy to produce excitation (the minimum energy required to excite a PAG is call the PAG excitation energy, E_{excit}). PAGs in an electronically excited state are converted to acid with a probability given by the PAG quantum efficiency (ϕ_{PAG}). Note that for this excitation model, electrons are not trapped by the PAG but instead transfer energy to the PAG via the continuous slowing down approximation and then keep traveling. Eventually, the electron reaches a kinetic energy that is insufficient to cause PAG conversion and is assumed to recombine with the ionized polymer. Details of this exposure model have been previously published.[2] Additionally, an inert trapping mechanism is included: when the electron energy reaches the inert trapping threshold energy (T_{inert}), the electron is trapped with 100% probability and without causing further excitation. Note that if this inert trapping energy is lower than the lowest energy that could possibly cause excitation, then the inert trapping will not impact PAG kinetics.

The first-order nature of this excitation mechanism has been derived as follows.[8] Consider first the generation of photoelectrons. Letting $[e^-]$ be the number density of photoelectrons generated by exposure, a standard kinetic rate equation for photoelectron generation will be similar to the standard rate equation for direct photon resist exposure[9]

$$\frac{d[e^-]}{dt} = \alpha\phi_e I\left(\frac{\lambda}{hc}\right), \tag{1}$$

where t is the exposure time, I is the intensity of light, α is the resist absorption coefficient, λ is the vacuum wavelength, h is Planck's constant, and c is the vacuum speed of light. Solving this rate equation,

$$[e^-] = \alpha\phi_e E\left(\frac{\lambda}{hc}\right), \tag{2}$$

where E is the exposure dose ($= It$). The total number of electrons, including secondaries, will be a multiple of this value, with k_s as the secondary electron yield

$$[e_s^-] = k_s[e^-]. \tag{3}$$

Now, let these photoelectrons and secondary electrons migrate through the resist, occasionally colliding with a PAG to generate an acid. Since the electrons are not trapped in this collision, their concentration is unaffected by the PAG reaction. A standard second-order rate equation based on collision kinetic theory would look like

$$\frac{dP}{dt} = v\phi_{\text{PAG}}\sigma_{e-\text{PAG}}[e_s^-]P, \tag{4}$$

where $\sigma_{e\text{-PAG}}$ is the reaction cross-section between the electron and the PAG and v is the velocity of the electron. Note that t in this equation is the time the electron spends moving about the resist and reacting with PAGs. Combining Eqs. (2) and (4) and integrating,

$$P = P_0 e^{-K}, \text{ where } K = v\phi_{\text{PAG}}\sigma_{e-\text{PAG}}\int_0^\infty [e_s^-]\,dt. \tag{5}$$

Defining the lifetime τ of the electron as

$$\tau = \frac{1}{[e_s^-](t=0)}\int_0^\infty [e_s^-]\,dt, \tag{6}$$

and noting that the photoelectron density at $t=0$ is given by Eq. (2), we have

$$K = CE = \alpha\phi_e\phi_{\text{PAG}}\sigma_{e-\text{PAG}}E\left(\frac{\lambda}{hc}\right)k_s v\tau, \tag{7}$$

where C is the Dill exposure rate constant. Letting $d_e = k_s v\tau$, this quantity can be thought of as the mean effective path length of the photoelectron traveling in the resist. It is the path length of the electron during which it still has enough energy to excite a PAG. If the photoelectron generates secondary electrons, then this distance can be interpreted as the mean sum of the path lengths of all the electrons. The final result is

$$C = d_e\phi_e\alpha\phi_{\text{PAG}}\sigma_{e-\text{PAG}}\left(\frac{\lambda}{hc}\right). \tag{8}$$

In a previous study, simulations with the PROLITH SRM X3.2 excitation model matched this result when[4]

$$d_e = 4.75\,\text{nm}\left(1 - \frac{IP}{110\,\text{eV}}\right), \quad \sigma_{e-\text{PAG}} = \pi(r - r_0)^2,$$
$$r_0 = 0.0084E_{\text{excit}}^2. \tag{9}$$

Thus, the simplified two-step kinetic exposure model presented in this section matches the overall results obtained from the more detailed mechanism embedded in the PROLITH SRM. Of course, the more detailed EUV exposure mechanism in PROLITH allows d_e and $\sigma_{e\text{-PAG}}$ to be expressed as a function of more fundamental scattering and reaction parameters. Also, the product $d_e\sigma_{e\text{-PAG}}$ can be interpreted as the mean effective volume of resist sampled by all the electrons that come from one absorbed photon (V_e). As

an example, if $r = 2\,\text{nm}$, $E_{\text{excit}} = 5\,\text{eV}$, and $IP = 10\,\text{eV}$, we have $d_e = 4.3\,\text{nm}$, $\sigma_{e\text{-PAG}} = 10.1\,\text{nm}^2$, and the mean effective volume is about $V_e = 43.5\,\text{nm}^3$. This volume multiplied by the PAG concentration is the mean number of PAGs that one photon has a chance to excite. For the $43.5\,\text{nm}^3$ effective volume and an initial PAG density of $0.3\,\text{nm}^{-3}$, there are 13 PAGs, on average, that could be excited by one photon at the beginning of exposure.

Often, the final result is expressed in terms of the relative acid concentration ($\langle h \rangle$, the mean acid concentration divided by the initial PAG concentration). For the first-order result predicted here,

$$\langle h \rangle = 1 - \frac{\langle P \rangle}{\langle P_0 \rangle} = 1 - e^{-C\langle E \rangle}. \tag{10}$$

In the version of PROLITH used in the previous study (version X3.2), the inert trapping threshold was fixed at $T_{\text{inert}} = 25\,\text{eV}$. In the latest version, this parameter can be varied and can be made as low as 10 eV. The influence of this parameter on the above results was studied using version X4.2. As an electron loses energy, it eventually has too little energy to be able to excite the PAG. If T_{inert} is below this minimum energy, then the parameter will not influence the resulting value of the exposure rate constant, C. Figure 1 shows the results of simulations where T_{inert} was varied and the percentage change in C determined (compared to $T_{\text{inert}} = 10\,\text{eV}$), as a function of the PAG excitation radius.

One of the most interesting aspects of an EUV resist is the possibility of an acid yield (the average number of generated acids per absorbed photon) greater than 1. Since the energy of one EUV photon (92 eV) far exceeds the minimum energy required to convert a PAG into an acid (on the order of 5 eV), each absorbed photon can potentially generate many acids. But for that to happen, there must be a sufficient number of unreacted PAGs in the neighborhood of the absorption event. Consider the initial (low-dose) acid yield, Y_0, defined as

$$Y_0 = \lim_{\text{dose}\to 0}\left(\frac{\#\,\text{acids generated}}{\#\,\text{absorbed photons}}\right). \tag{11}$$

This initial acid yield for a first order exposure mechanism will be

$$Y_0 = \frac{C}{\alpha}\left(\frac{hc}{\lambda}\right)P_0 = d_e\phi_e\phi_{\text{PAG}}\sigma_{e-\text{PAG}}P_0 = \phi_e\phi_{\text{PAG}}V_eP_0. \tag{12}$$

Thus, the excitation mechanism used here, like any first-order model, will show a linear increase in acid yield with PAG loading.

III. HIGGINS COMPETING TRAPS MODEL

Higgins *et al.*[10] proposed a simple continuum trapping model for EUV resist exposure where the PAG competes with inert components in the resist to trap an electron.

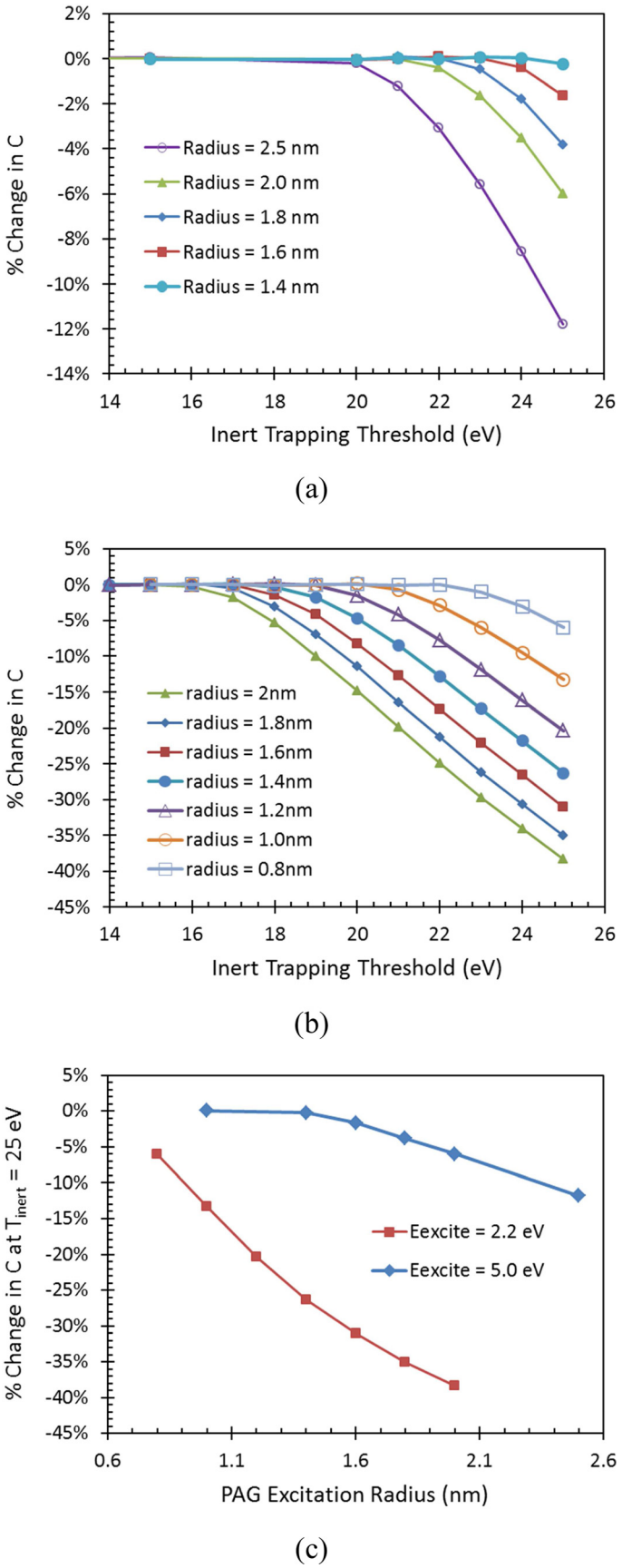

FIG. 1. (Color online) Percent change in the exposure rate constant C as the inert trapping threshold is increased from 10 eV, as a function of the PAG excitation radius, with (a) $E_{\text{excite}} = 5\,\text{eV}$ and (b) $E_{\text{excite}} = 2.2\,\text{eV}$. The percent change in C as T_{inert} is changed from 10 to 25 eV is shown in (c).

Photon absorption leads to photoionization, and photoelectrons can create secondary electrons, a reaction that is presumed first order with rate constant k_1. Electrons can be trapped by an unchanging concentration of inert traps, with rate constant k_2. Electrons can also be trapped by PAG, in a reaction that is first order in both electron concentration and PAG concentration with rate constant k_3. The assumption of a steady state concentration of electrons, $[e^-]$, leads to

$$\frac{d[e^-]}{dt} = 0 = k_1 I - k_2[e^-] - k_3[e^-][\mathrm{PAG}]. \tag{13}$$

Solving for $[e^-]$, the rate of PAG reaction becomes

$$\frac{d[\mathrm{PAG}]}{dt} = -k_3[e^-][\mathrm{PAG}] = -\frac{\left(\frac{k_3 k_1}{k_2}\right) I[\mathrm{PAG}]}{1 + \left(\frac{k_3}{k_2}\right)[\mathrm{PAG}]}. \tag{14}$$

Letting $P = [\mathrm{PAG}]$, this rate equation can be solved with the initial condition of $P(t=0) = P_0$. Letting $y = P/P_0$, $a = (k_3/k_2)P_0$, and $k_c = (k_3 k_1/k_2)$,

$$aye^{ay} = ae^{(a-k_c E)}, \tag{15}$$

where E is the exposure dose, $E = It$. This transcendental equation is solved using the Lambert W function:

$$ay = W\left(ae^{(a-k_c E)}\right). \tag{16}$$

Thus, the relative acid concentration $h = 1 - y$ becomes

$$h = 1 - \frac{1}{a} W\left(ae^{(a-k_c E)}\right). \tag{17}$$

The Lambert W function is plotted in Fig. 2 and has the following useful identities:

$$W(ae^a) = a, \quad W'(z) = \frac{W}{z(1+W)}, \quad \lim_{z\to 0} W(z) = z. \tag{18}$$

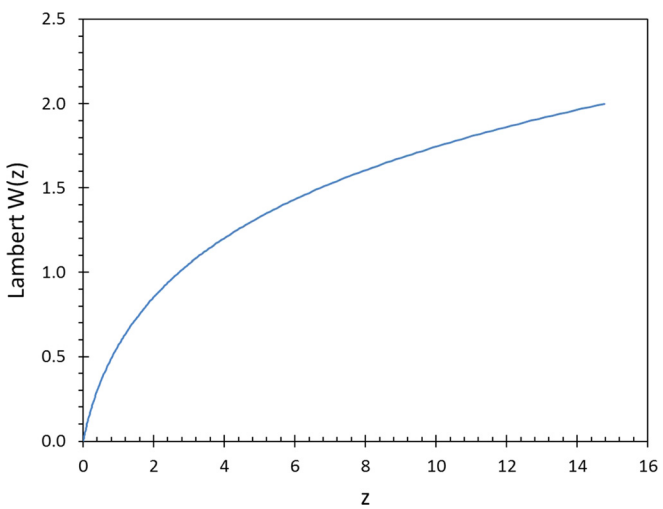

FIG. 2. (Color online) Plot of the Lambert W function.

The Higgins competing traps model becomes first order when $a \ll 1$ (that is, for small PAG loading). Using a Taylor expansion of the Lambert W function for this case,

$$h \approx 1 - \frac{e^{(a-k_c E)}}{1 + ae^{(a-k_c E)}} \approx 1 - e^{-k_c E}. \tag{19}$$

A comparison between the Higgins model and a first order rate equation for the case of $a = 1$ is shown in Fig. 3. It is clear that a measurement of acid concentration versus dose is unlikely to supply sufficient precision to differentiate between the Higgins model and first-order behavior. In fact, the Higgins model $h(E)$ curve can be well matched by a first-order kinetic $h(E)$ curve when

$$C = \frac{k_c}{1 + a/2}. \tag{20}$$

The slope of the $h(E)$ curve for the Higgins model is

$$\frac{dh}{dE} = k_c\left(\frac{1-h}{1 + a(1-h)}\right). \tag{21}$$

For a first-order reaction, the Dill exposure rate constant C is the slope of the $h(E)$ curve as the dose goes to zero. For the Higgins competing traps model, this "C-like" behavior is

$$\lim_{E\to 0}\frac{dh}{dE} = \frac{k_c}{1+a} = \frac{k_1 k_3}{k_2 + k_3 P_0}. \tag{22}$$

Further, the initial acid quantum yield will be

$$Y_0 = \frac{P_0}{\alpha}\left(\frac{hc}{\lambda}\right)\lim_{E\to 0}\left(\frac{h}{E}\right) = \frac{P_0}{\alpha}\left(\frac{hc}{\lambda}\right)\left(\frac{k_c}{1+a}\right). \tag{23}$$

Another useful form of this equation is

$$Y_0 = Y_{\max}\left(\frac{P_0}{P_c + P_0}\right), \quad Y_{\max} = \frac{k_1}{\alpha}\left(\frac{hc}{\lambda}\right), \quad P_c = \frac{P_0}{a} = \frac{k_2}{k_3}, \tag{24}$$

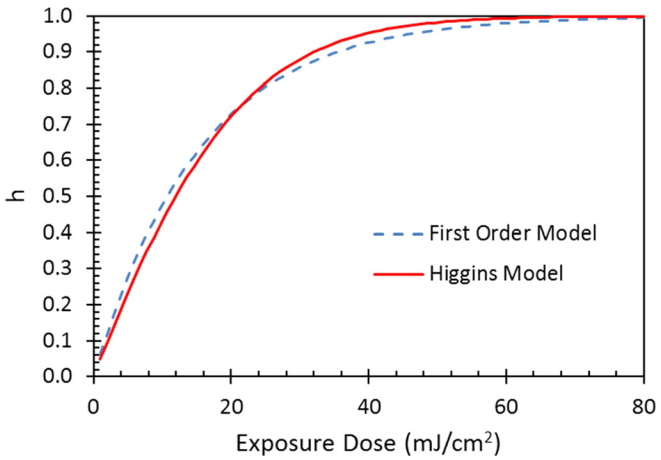

FIG. 3. (Color online) Comparison of the Higgins competing trap model ($a = 1$, $k_c = 0.1$ cm^2/mJ, solid line) to a first-order rate equation ($C = 0.065$ cm^2/mJ, dashed line).

where P_c is the crossover PAG loading. For $P_0 \ll P_c$, acid yield increases linearly with PAG loading. For $P_0 \gg P_c$, yield saturates at the maximum value $Y_{\max}$. Thus, this behavior of the Higgins competing trap model differs from a first order model at sufficiently high PAG loading.

The case of low levels of inert trapping is also interesting. Letting $k_2 \to 0$, the steady-state assumption invoked above means that the generation of acid becomes limited only by the generation of electrons, and every electron eventually finds a PAG and forms an acid. Since the generation of acid will eventually become limited by the availability of PAG, the steady-state assumption will always become invalid at a high enough dose. Still, at low doses, it may be a reasonable assumption. For this case, solution to the rate equation becomes

$$h = \frac{k_1}{P_0} E. \tag{25}$$

The C-like parameter is then k_1/P_0. In this regime, the low-dose yield is always $Y_{\max}$, independent of PAG loading.

IV. PROLITH SRM TRAPPING MODEL CONTUINUUM APPROXIMATION

PROLITH x4.2 has implemented a trapping mechanism to complement the excitation mechanism described above. In this trapping mechanism, any electron within a specific energy range that travels within the PAG trapping radius of a PAG molecule will be trapped with 100% efficiency. The energy of electrons that can be trapped by a PAG falls between the PAG trapping threshold energy (T_{PAG}) and the inert trapping threshold (T_{inert}). Once a PAG traps an electron, it releases an acid with probability ϕ_{trap}. Note that this mechanism differs from the Higgins competing traps model since here the inert species traps the acid outside of the energy range that the PAG can trap an electron, and thus does not compete with the PAG for the electron. Below we will derive the continuum kinetic model that complements the stochastic trapping model in PROLITH.

The rate of PAG conversion will be proportional to the probability that an electron will be trapped by a PAG. Consider an electron that travels an effective distance d_e while within the energy range from T_{PAG} to T_{inert}. As with the excitation model, the effective volume sampled by the electron (or electrons, considering the possibility of secondary generation), while within the proper energy range, will be $V_e = d_e \sigma_{e\text{-PAG}}$. If an electron encounters a PAG molecule within this volume, it will always be trapped. Thus, the probability of an electron being trapped is one minus the probability that there will be no PAG molecules within this volume.

The spatial distribution of PAG molecules is assumed to follow a Poisson probability distribution. The probability of finding exactly n PAG molecules within a volume V_e will be

$$\text{Prob}(n) = \frac{(PV_e)^n}{n!} e^{-PV_e}, \tag{26}$$

where P is the mean concentration of PAG molecules. Thus, the probability of an electron being trapped will be

$$\text{Probability of Trapping} = 1 - \text{Prob}(n = 0) = 1 - e^{-PV_e}. \tag{27}$$

The rate of PAG reaction will be proportional to this probability

$$\frac{dP}{dt} = -k_4[e^-](1 - e^{-PV_e}). \tag{28}$$

Recalling Eqs. (2) and (6), this rate equation can be solved for P and for the relative acid concentration h.

$$\langle h \rangle = \phi_{\text{trap}} \left(1 - \frac{1}{P_o V_e} \ln[1 + (e^{P_o V_e} - 1)\, e^{-k_5 V_e \langle E \rangle}] \right), \tag{29}$$

where $k_5 = k_4 \tau \alpha \phi_e \left(\frac{\lambda}{hc} \right)$.

The low-dose behavior of this model is revealing. When $k_5 V_e E \ll 1$,

$$\langle h \rangle \approx \phi_{\text{trap}} \frac{k_5}{P_o} (1 - e^{-P_o V_e}) \langle E \rangle. \tag{30}$$

In general, $P_0 V_e$, the average number of PAG molecules that could be encountered by all the electrons that come from one absorbed photon, will be much greater than one. For this condition, the low-dose behavior becomes

$$\langle h \rangle \approx \phi_{\text{trap}} \frac{k_5}{P_o} \langle E \rangle. \tag{31}$$

Thus, the C-like term is k_5/P_0. Note the resemblance to Eq. (25), the Higgins model at low doses for the case of no traps competing with the PAG trapping, where $k_5 \phi_{\text{trap}}$ here resembles k_1 of the Higgins model. When $P_0 V_e \gg 1$, Eq. (29) becomes

$$\begin{aligned} \langle h \rangle &\approx \phi_{\text{trap}} \left(1 - \frac{1}{P_o V_e} \ln[1 + e^{V_e (P_0 - k_5 \langle E \rangle)}] \right) \\ &= \phi_{\text{trap}} \left(1 - \frac{1}{P_o V_e} \ln\left[1 + e^{V_e P_0 \left(1 - \frac{k_5}{P_0} \langle E \rangle \right)} \right] \right). \end{aligned} \tag{32}$$

The PROLITH trapping model has three parameters, ϕ_{trap}, k_5, and V_e. The impact of ϕ_{trap} is obvious, and Fig. 4 shows the impact of the remaining two parameters on the $h(E)$ curve. It is clear that k_5/P_0 controls the initial slope of the curve, and $V_e P_0$ controls the shape of the curve as it transitions from linear to saturated. When $V_e P_0 \ll 1$, the behavior becomes first-order

$$\langle h \rangle \approx \phi_{\text{trap}} (1 - e^{-k_5 V_e \langle E \rangle}). \tag{33}$$

When $V_e P_0 \gg 1$ the $h(E)$ curve is linear until it reaches saturation, then quickly flattens.

The low-dose slope of the $h(E)$ curve for the PROLITH trapping model is

$$\lim_{E \to 0} \frac{dh}{dE} = \phi_{\text{trap}} \frac{k_5}{P_o} (1 - e^{-P_o V_e}). \tag{34}$$

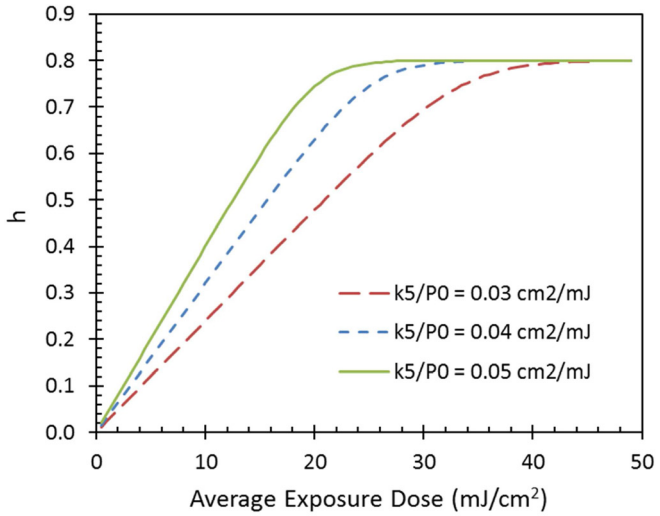

(a)

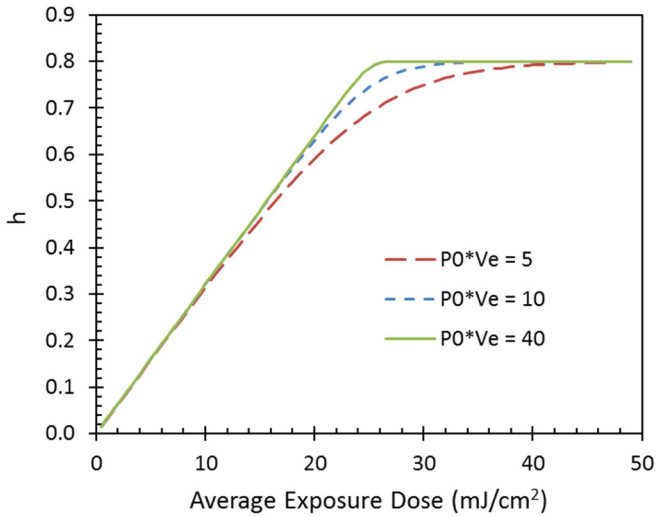

(b)

FIG. 4. (Color online) PROLITH trapping model (with $\phi_{trap} = 0.8$) with (a) $V_e P_0 = 10$ and varying k_5/P_0, and (b) $k_5/P_0 = 0.04$ cm^2/mJ and varying $V_e P_0$.

The initial acid quantum yield is

$$Y_0 = \frac{P_0}{\alpha}\left(\frac{hc}{\lambda}\right)\lim_{E\to 0}\left(\frac{h}{E}\right) = \frac{k_5}{\alpha}\left(\frac{hc}{\lambda}\right)(1 - e^{-P_0 V_e}). \quad (35)$$

As the PAG loading increases, the low-dose acid yield quickly saturates at $Y_{max} = \frac{k_5}{\alpha}\left(\frac{hc}{\lambda}\right)$. Since we expect that $V_e P_0 \gg 1$ for normal PAG loadings, the result is an acid yield that is essentially independent of PAG loading.

V. PROLITH SRM TRAPPING MODEL SIMULATIONS

To test the derivations from the previous section, PROLITH X4.2 was run with the trapping mechanism turned on and the excitation mechanism turned off. For each set of input parameters, $h(E)$ was simulated for 100 dose values. At least 100 trials were then averaged together and the resulting data fit to Eq. (29) to extract k_5 and V_e. Figure 5 shows a typical example (note that the dose plotted is the dose averaged through the thickness of the 10-nm film). The fit of the continuum model is quite good, though not perfect. Systematic residuals are as large as 0.01, which means the continuum model prediction of mean acid concentration matches the stochastic PROLITH simulations to within 1% of the initial PAG concentration.

Next, the PROLITH input parameters were varied and the continuum trapping model parameters extracted for each case (using 100 exposure doses and the average of 100 trials). For the baseline parameters as shown in Fig. 5, using 100 trials produces a value of k_5 with 0.1% standard deviation and V_e with 1% standard deviation. Varying ϕ_{PAG} from 0.7 to 1.0 had no impact on k_5 or V_e, as expected. The impact of PAG reaction radius r, PAG trapping threshold energy T_{trap}, and PAG loading P_0 are shown in Figs. 6–8, respectively. In all cases, the continuum model fit the stochastic

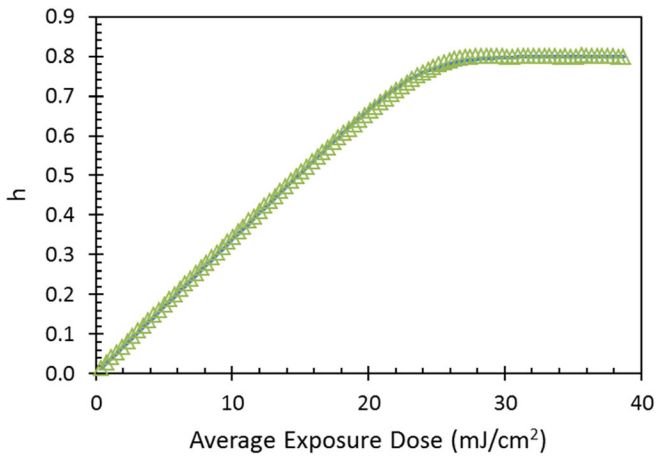

(a)

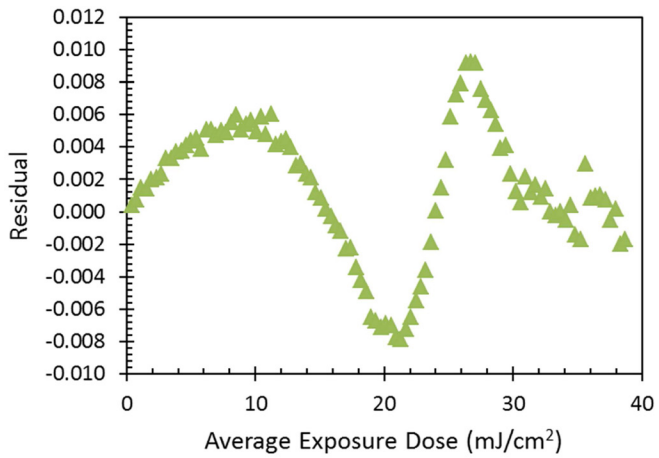

(b)

FIG. 5. (Color online) PROLITH SRM X4.2 trapping model simulations (with $\phi_{trap} = 0.8$, $\phi_e = 0.9$, $r = 2$ nm, $\alpha = 0.0065159\,\text{nm}^{-1}$, $T_{trap} = 15$ eV, $T_{inert} = 10$ eV, $P_0 = 0.2\,\text{nm}^{-3}$, and 10 nm resist thickness): (a) PROLITH simulations (symbols) and best fit continuum model (solid line) and (b) residuals comparing continuum model to PROLITH simulations for the average of 1000 trials.

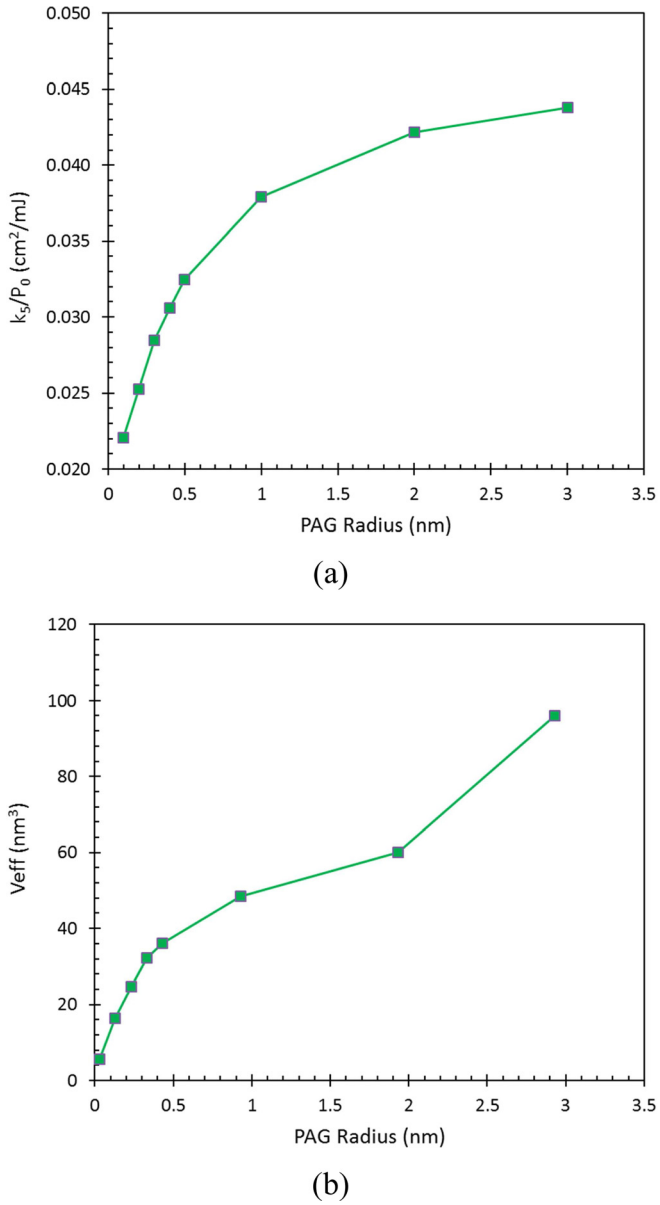

FIG. 6. (Color online) Continuum model fits to the PROLITH SRM X4.2 trapping model simulations (with $\phi_{trap}=0.8$, $\phi_e=0.9$, $r=$variable, $\alpha=0.0065159\,nm^{-1}$, $T_{trap}=15\,eV$, $T_{inert}=10\,eV$, $P_0=0.2\,nm^{-3}$, 10 nm resist thickness, the average of 100 trials): (a) k_5/P_0 and (b) V_e.

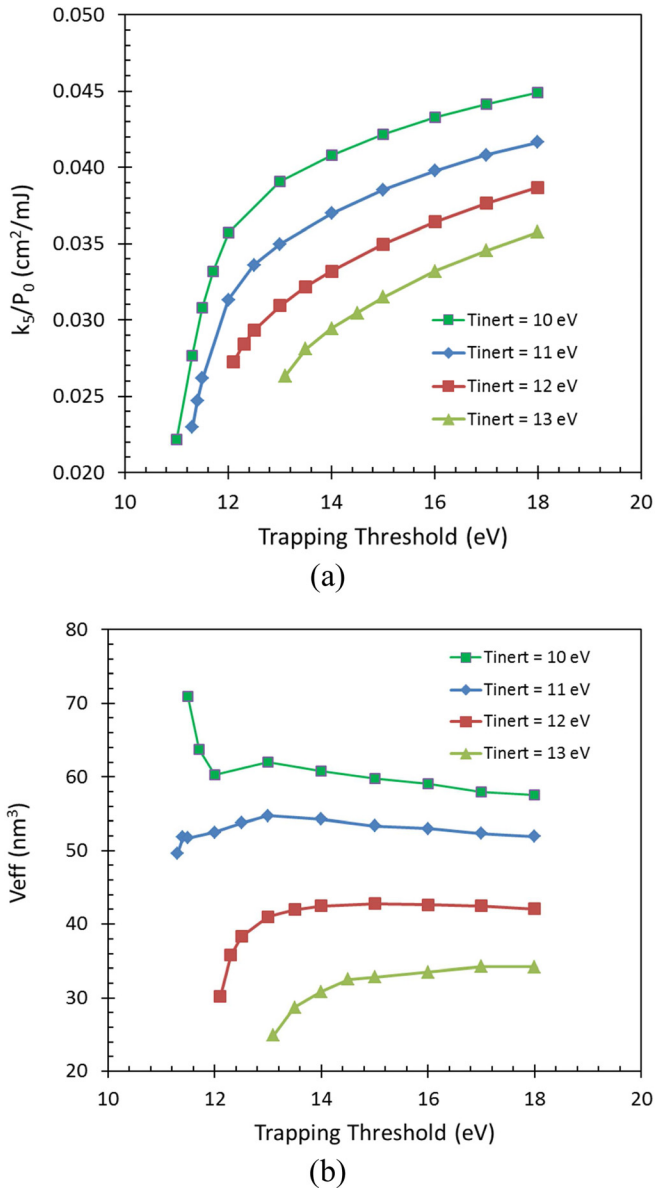

FIG. 7. (Color online) Continuum model fits to the PROLITH SRM X4.2 trapping model simulations (with $\phi_{trap}=0.8$, $\phi_e=0.9$, $r=2\,nm$, $\alpha=0.0065159\,nm^{-1}$, $T_{trap}=$variable, $T_{inert}=10\,eV$, $P_0=0.2\,nm^{-3}$, 10 nm resist thickness, the average of 100 trials): (a) k_5/P_0 and (b) V_e.

simulation results to about the same degree of error as shown in Fig. 5.

VI. DISCUSSION AND CONCLUSIONS

Three different continuum mechanisms for EUV resist exposure have been discussed: an excitation mechanism, the Higgins competing traps mechanism, and a PAG trapping mechanism (without competition). Further, a stochastic excitation model and a stochastic PAG trapping model, as implemented in PROLITH X4.2, were compared to their continuum counterparts. The stochastic excitation model (predicting the mean acid concentration) matches the continuum (first order) excitation model exactly. The stochastic PAG trapping model matches the continuum PAG trapping model fairly well, but with some systematic differences. The nature of those differences has yet to be explored.

One of the goals of this work is to compare the predictions made by these three different mechanisms to look for differences. Sufficiently different predictions could be compared to experiment, possibly allowing one mechanism to rise above the others in utility. Three possible experiments can be compared: the $h(E)$ curve, the slope of the $h(E)$ curve versus PAG loading, and acid yield versus PAG loading.

The $h(E)$ curves for the first-order excitation mechanism and the Higgins competing traps mechanism are too similar to be differentiated experimentally for normal levels of experimental uncertainty. For the case of large P_0V_e, the PAG trapping mechanism has a sufficiently different shape (linear until almost all of the PAG has been used up) that it may be experimentally possibly to validate or invalidate its use.

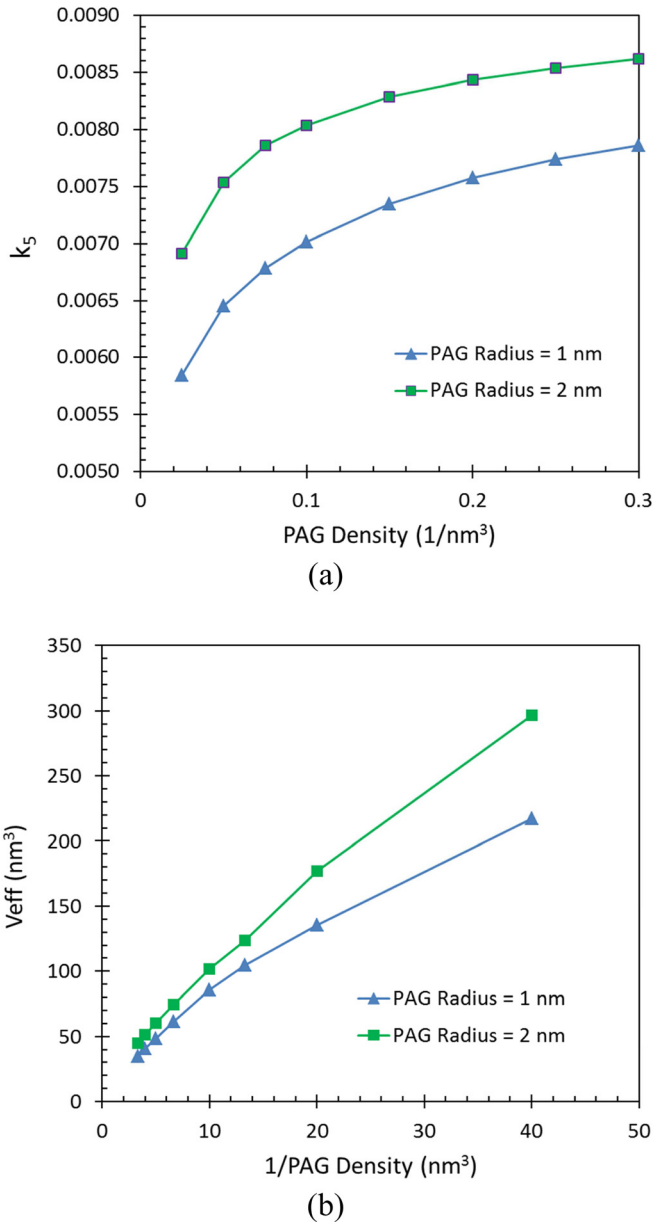

FIG. 8. (Color online) Continuum model fits to the PROLITH SRM X4.2 trapping model simulations (with $\phi_{trap} = 0.8$, $\phi_e = 0.9$, $r = 1$ and 2 nm, $\alpha = 0.0065159\,nm^{-1}$, $T_{trap} = 15\,eV$, $T_{inert} = 10\,eV$, $P_0 =$ variable, 10 nm resist thickness, the average of 100 trials): (a) k_5 and (b) V_e.

The initial slope of the $h(E)$ curve produces a C-like parameter that has different variation with respect to PAG loading for the different mechanisms. For the first-order excitation mechanism, this slope is independent of PAG loading. For the Higgins competing traps mechanism and the PAG trapping mechanism, this slope varies inversely with P_0, though in somewhat different ways. Thus, variation of the C-like parameter with PAG loading should allow the excitation mechanism to be differentiated from the trapping mechanisms. It may be difficult, however, to see the difference between the two trapping mechanisms, depending on whether reliable data can be obtained at very low PAG loadings.

The three mechanisms also produce different predictions of acid yield as a function of PAG loading. The first-order excitation mechanism predicts a yield that increases in direct proportion to P_0. The Higgins competing traps mechanism predicts an initial linear behavior, saturating to a maximum yield at higher PAG loadings. The PAG trapping mechanism (without competition) predicts a quick exponential rise to a constant yield as a function of P_0. Thus, it seems possible that this experiment could help to differentiate between the three mechanisms. There is a potential complication, though. A resist that reacts according to the excitation mechanism at higher electron energies (above 20 eV, for example) and reacts according to the PAG trapping mechanism at lower electron energies (below 15 eV, for example) would exhibit behavior that is very similar to the Higgins competing traps mechanism.

A note of caution is in order when considering the experimental impact of PAG loading. All of the models in this paper assume simple behavior with increasing PAG loading: PAG is always "evenly" distributed throughout the film (following a Poisson distribution), with no clustering or z-dependence of the concentration. An experimental film that does not adhere to this assumption may produce data that is difficult to analyze.

The topic of this paper could certainly benefit from future work. Other mechanisms (besides the three described here) could be explored. Other lithographic predictions, such as dose-to-clear and dose-to-size as a function of PAG loading, might also provide differentiable experiments. And finally, it will be extremely interesting to use the PROLITH stochastic PAG trapping model to predict not only the mean acid concentration as a function of dose (and other model parameters) but the standard deviation of the acid concentration as well. An understanding of the variance of acid production is essential to a complete understand of line-edge roughness mechanisms in EUV lithography.

[1]T. Kozawa and S. Tagawa, Jpn. J. Appl. Phys. **49**, 030001 (2010).
[2]J. J. Biafore, M. D. Smith, D. Blankenship, S. A. Robertson, E. van Setten, T. Wallow, Y. Deng, and P. Naulleau, Proc. SPIE **7636**, 76360R-1 (2010).
[3]R. J. Hawryluk, A. M. Hawryluk, and H. I. Smith, J. Appl. Phys. **45**, 2551 (1974).
[4]M. Dapor, *Electron-Beam Interactions with Solids: Application of the Monte Carlo Method to Electron Scattering Problems* (Springer-Verlag, Berlin, 2003).
[5]C. J. Tung, J. C. Ashley, and R. H. Ritchie, IEEE Trans. Nucl. Sci. **26**, 4874 (1979).
[6]J. C. Ashley, C. J. Tung, and R. H. Ritchie, IEEE Trans. Nucl. Sci. **25**, 1566 (1978).
[7]T. Inagaki, E. T. Arakawa, R. N. Hamm, and M. W. Williams, Phys. Rev. B **15**, 3243 (1977).
[8]C. A. Mack, J. W. Thackeray, J. J. Biafore, and M. D. Smith, J. Micro/Nanolith. MEMS MOEMS **10**, 033019 (2011).
[9]Chris A. Mack, *Fundamental Principles of Optical Lithography: The Science of Microfabrication* (Wiley, London, 2007), pp. 195–197.
[10]C. D. Higgins, C. R. Szmanda, A. Antohe, G. Denbeaux, J. Georger, and R. L. Brainard, Jpn. J. Appl. Phys. **50**, 036504 (2011).